Impact of Antenna Patterns and Orientations in Heterogeneous LTE-Advanced Networks

Zuhanis Mansor, Evangelos Mellios, Andrew Nix, Joe McGeehan, and Geoffrey Hilton

Centre for Communications Research, Department of Electrical & Electronic Engineering, University of Bristol
Merchant Venturers Building, Woodland Road, Bristol, BS8 1UB, Bristol, United Kingdom
Anis.Mansor@bristol.ac.uk

***Abstract*- Antenna configurations and orientations are known to have a major influence on the performance of a wireless communications link. In this paper we study the impact of antenna patterns and orientations on the downlink of an OFDMA LTE-Advanced system. We consider a heterogeneous network (HetNet) comprising a large macrocell with a single picocellular underlay. The spatial and temporal characteristics of the radio channel are modelled using 3D ray-tracing and combined with appropriately oriented complex polarmetric antenna patterns. The handset is rotated in the azimuth and elevation planes to evaluate performance sensitivity. User performance is analysed in terms of data throughput, received power, bit error rate and packet error rate. The received bit mutual information rate (RBIR) abstraction technique is applied for all modulation and coding schemes (MCS) to determine the optimal physical layer throughput. Results show that antenna pattern and orientation significantly influence user performance, especially in the macrocell.**

Index Terms—HetNets, Cellular networks, OFDMA.

I. INTRODUCTION

Mobile data traffic is expected to grow at a compound annual growth rate (CAGR) of 92% from 2010 to 2015, reaching 6.3 exabytes per month by 2015 [1]. As illustrated in Fig. 1, mobile data traffic for smartphones, laptops and tablets is predicted to double each year from 2011 to 2015 [1]. Data traffic demands in cellular networks are growing rapidly and significant improvements are now required in spectral efficiency.

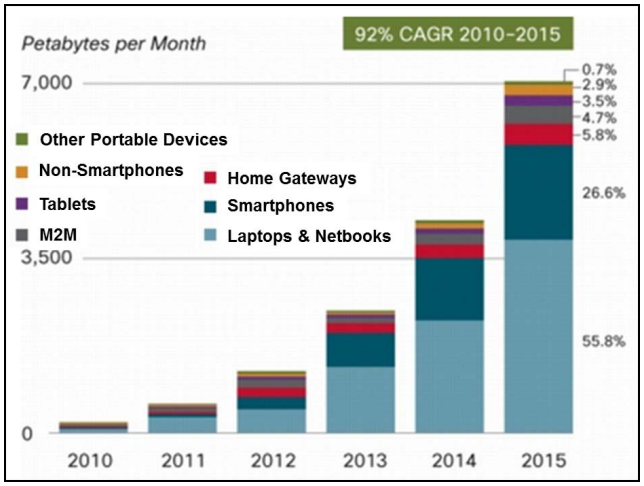

Figure 1: The global mobile traffic forecast [1]

The initial deployment of Long Term Evolution (LTE) networks consists of macro base stations to provide wide area coverage in urban regions. To enhance capacity, one solution is to complement the macro layer with a number of lower power pico base stations, thereby creating a heterogeneous network. To achieve high throughputs and capacities in an LTE system we must carefully design both the base station and user equipment (UE) antennas. UE orientation can have a significant impact on performance. An analysis of the impact of antenna tilt on LTE coverage and capacity was analysed in [2] where system performance was affected by different combinations of electrical and mechanical tilt. The downlink performance of an 802.11n system with antenna pattern orientation was also addressed in [3].

In this paper, we extend previous work by considering a macro/pico LTE deployment (i.e. a heterogeneous network or HetNet). More specifically we focus on the LTE downlink and model the detailed spatial and temporal multipath structure using a 3D ray tracing model. The UE is tilted in the x-z plane at 0°, 45° and 90° (denoted as case 1, case 2 and case 3 respectively) as shown in Fig. 2. For each case the UE is then rotated through 360° in the x-y plane (in steps of 90°) in order to evaluate azimuth orientation sensitivity.

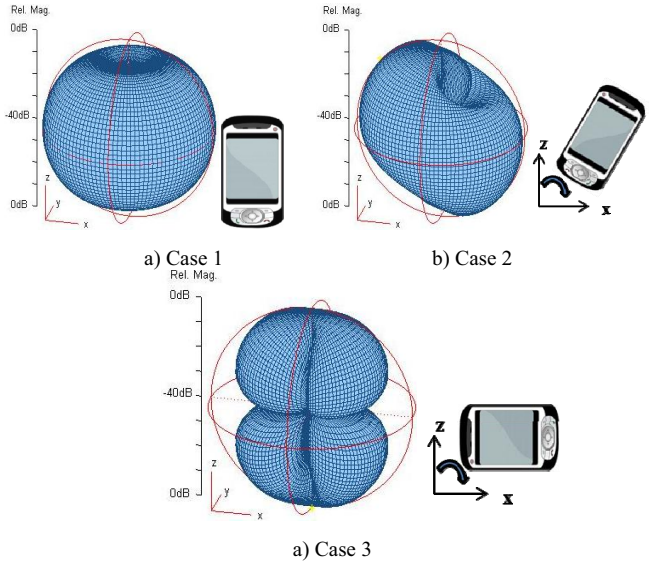

Figure 2: The effect of elevation tilt on UE vertical polarisation, a) 0° elevation tilt (Case 1), b) 45° elevation tilt (Case 2) and c) 90° elevation tilt (Case 3) from vertical respectively (0° Azimuth Rotation).

The remainder of the paper is structured as follows. In section II, the system model for OFDMA is presented. Test scenarios and antenna configurations are given in section II. User performance evaluation is presented and discussed in section IV. Results are presented and discussed in section IV. Section V concludes the paper.

II. System Model

Fig. 3 shows the transmitter and receiver structure for the downlink of an LTE single antenna system. Orthogonal Frequency Division Multiple Access (OFDMA) has been adopted as the downlink transmission scheme in the 3rd Generation Partnership Project (3GPP) LTE standard [4]. OFDMA is a multiple access scheme based on Orthogonal Frequency Division Multiplexing (OFDM) where data is transmitted to different users on different subcarriers. It is suitable for high data rate transmission in wideband wireless systems due to its high spectral efficiency and good immunity to multipath fading.

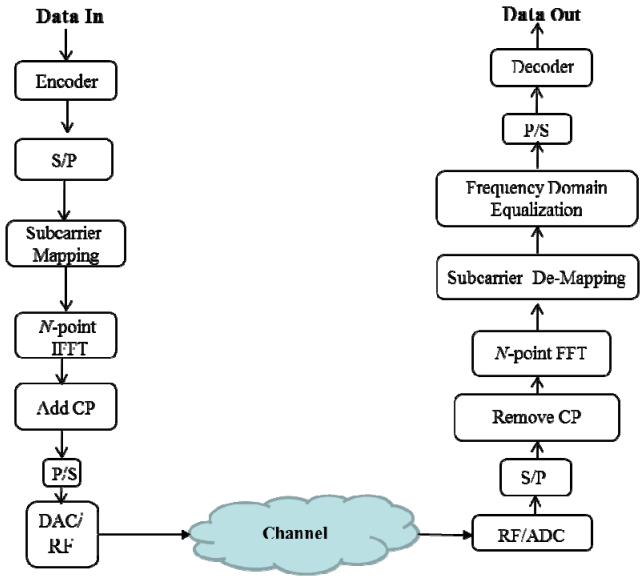

Figure 3: SISO model of a coded OFDMA system in HetNet Scenario.

A baseband LTE link level simulator has been implemented in MATLAB in order to investigate the link level performance of the LTE downlink. The OFDMA simulation parameters are defined based on the latest 3GPP TR 36.8414 standard [4]. Table I shows the key parameters of the LTE OFDMA downlink system.

TABLE 1: Parameters for LTE OFDMA

System Parameters	Specifications
Carrier Frequency	2 GHz
Transmission Bandwidth	10 MHz
Time Slot/Sub Frame Duration	0.5 ms /1 ms
Subcarrier Spacing	15 kHz
Sampling Frequency	15.36 MHz (4 x 3.84 MHz)
IFFT size	1024
Number of Occupied Subcarrier	600
Number of OFDMA symbols per time slot (Short CP)	7
CP Length (µs/samples)	(4.69/72) x 6, (5.21/80) x 1
Channel Knowledge	Perfect

In this paper, an LTE FDD system with a 10 MHz bandwidth is assumed. PHY layer throughput is used as the main metric for comparison. A target PER of 10% or less and a noise floor of -94.5dBm are assumed in the receiver [5]. In order to perform link-level analysis in an efficient and scalable way, a PHY layer abstraction technique is required. In this paper, the Received Bit Mutual Information Rate (RBIR) abstraction technique is applied to choose the optimal MCS. RBIR abstraction has been used in [6] and is fully described in [7][8]. This technique has been thoroughly validated against our LTE link-level simulator in order to validate the accuracy of the RBIR abstraction engine (see Fig. 4).

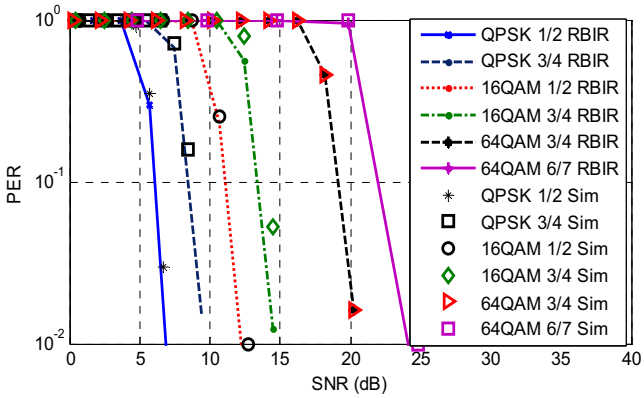

Figure 4: Validation for wideband channel

III. Test Scenarios and Antenna Configuration

Our HetNet scenario consists of a large macro base station and a single pico base station. Six user terminals are located in both the macrocell (UE-Macro) and picocell (UE-Pico) as shown in Fig.5. Analysis is performed at 2.6GHz with base station transmit powers of 43dBm and 30dBm respectively for the Macro-eNB and Pico-eNB. For each location, a set of 1000 channel snap-shots are considered to ensure statistical accuracy. The macro base station uses a macro evolved node-B (Macro-eNB), while the pico base station uses a pico evolved node-B (Pico-eNB). The mobile stations or handsets are denoted as user equipment (UE).

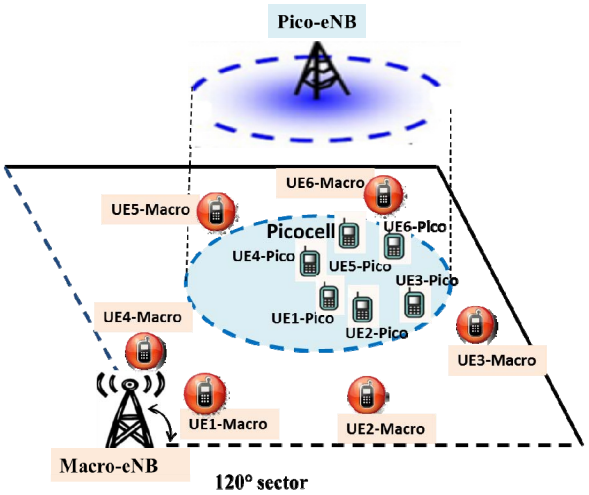

Figure 5: Heterogeneous network topology utilizing a mix of high power (macro) and low power (pico) base stations; analysis is performed at 2.6GHz with a transmit power of 43dBm and 30dBm for the Macro-eNB and Pico-eNB respectively.

The SISO channel between the Macro-eNB, Pico-eNB and each UE is modelled as the spatial convolution of the antenna patterns with the spatial and temporal multipath components from an 3D outdoor ray-tracer [9]. This deterministic approach is preferred over the standardized SCM 3GPP LTE channel model [10] since the latter makes several simplifying assumptions. These include: i) no consideration of a picocell environment, ii) simplified angle spread distributions, iii) propagation restricted to the azimuth plane, iv) no mechanism for modelling specific antenna patterns, and v) highly simplified polarization modelling.

In order to compute a statistically valid set of wideband channel matrices suitable for OFDMA modelling, the procedure reported in [13] was followed. Point-source ray-tracing was performed from the eNB to each UE location. This provides information on the amplitude, phase, time delay, angle-of-departure (AoD) and angle-of-arrival (AoA) of each multipath component (MPC). The complex gain of each MPC was adjusted according to the transmitting/receiving antenna *E*-field pattern response for the corresponding AoD/AoA and polarization. The double-directional time-invariant channel impulse response for a link is given by equation (2) [10].

$$h(\tau,\Omega_{AoD},\Omega_{AoA}) = \sum_{l=1}^{L} h_l(\tau,\Omega_{AoD},\Omega_{AoA}) = \\ = \sum_{l=1}^{L} \mathbf{E}_l \delta(\tau-\tau_l)\delta(\Omega_{AoD}-\Omega_{AoD,l})\delta(\Omega_{AoA}-\Omega_{AoA,l}) \quad (1)$$

where $$\mathbf{E}_l = \begin{bmatrix} E_{Tx}^V \\ E_{Tx}^H \end{bmatrix}^T \begin{bmatrix} a_l^{VV} e^{j\Phi_l^{VV}} & a_l^{VH} e^{j\Phi_l^{VH}} \\ a_l^{HV} e^{j\Phi_l^{HV}} & a_l^{HH} e^{j\Phi_l^{HH}} \end{bmatrix} \begin{bmatrix} E_{Rx}^V \\ E_{Rx}^H \end{bmatrix}$$

L represents the total number of MPCs. The l^{th} MPC has a complex amplitude $a_l^{XY} e^{j\Phi_l^{XY}}$ (2x2 matrix for all four polarization combinations), a time-of-flight τ_l and departure/arrival angles $\Omega_{AoD,l} / \Omega_{AoA,l}$. $E_{Tx}^{V/H} / E_{Rx}^{V/H}$ represents the vertical/horizontal polarization component of the transmitting and the receiving antenna *E*-field radiation pattern. The wideband channel frequency response $G(f) = [g_1, g_2, \ldots, g_N]$, where g_k represents the frequency domain SISO channel gain for the k^{th} subcarrier, which was computed using a 2048-point discrete Fourier transform (equation 3):

$$G(f) = F\{h(\tau_1 \Omega_{AoD} \Omega_{AoA})\} \quad (2)$$

To compute the expected average channel performance for a given link, we repeat this procedure for 1000 uncorrelated channel realizations. These are generated for a given link by applying a uniformly distributed [0,2π] random phase to each MPC between the eNB and UE. The Macro-eNB is located on the rooftop of a 30m tall building and employs a theoretically modelled vertically polarized directional antenna, as proposed in [11], down-tilted by 10°. The Pico-eNB is mounted on the outer wall of a building, 5m above the ground level. It utilizes a vertically polarized patch antenna, the pattern of which was measured in-situ in an anechoic chamber. Figs. 6 and 7 show the vertical polarization components of the Macro-eNB and the Pico-eNB antenna radiation patterns. The UE antenna is theoretically modelled as a vertically polarized Hertzian dipole [12], located 1.5m above the ground level. Fig. 8 and Table II illustrate the UE rotations used in this study. Table III presents the propagation characteristics for all the UE locations (0° orientation elevation and azimuth).

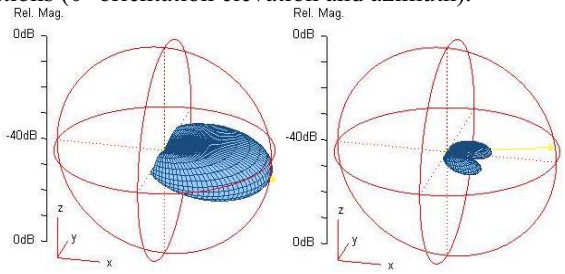

a) Vertical polarisation B) Horizontal polarisation

Figure 6: Macro-eNB antenna radiation patterns.

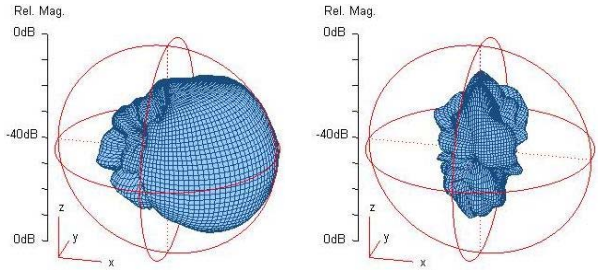

a) Vertical polarisation B) Horizontal polarisation

Figure 7: Pico-eNB antenna radiation patterns.

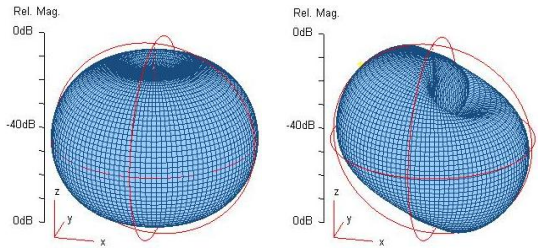

a. Case1 b. Case2

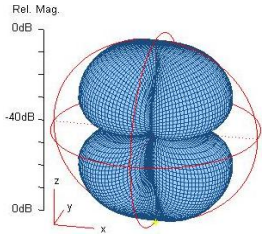

c. Case3

Figure 8: Effect of elevation tilt on user terminal (UE) vertical polarization component, a) Case 1, b) Case 2 and c) Case 3.

TABLE II: MODEL ROTATIONS FOR THE UE

Case	Elevation Tilt (x-z plane)	Azimuth Rotation (x-y plane)
1a/1b/1c/1d	0°	90°/180°/270°/360°
2a/2b/2c/2d	45°	
3a/3b/3c/3d	90°	

TABLE III: PROPAGATION CHARACTERISTICS OF 0° User Antenna Elevation Tilt and Azimuth Rotation in Macrocell/Picocell Scenario

Location	Distance from Base Station (m)	K-factor (dB)	Total Average Received Power (dBm)	RMS delay Spread (nsec)	Coherence Bandwidth (MHz)	Elevation AoA RMS Spread (degrees)
UE1	~108/~11	3.9/17.0	-35.2/-23.9	46.3/3.3	5.9/83.3	5.2/3.7
UE2	~500/~60	3.7/-0.8	-60.1/-67.9	104.9/109.6	2.6/2.5	2.0/5.5
UE3	~1020/~104	5.6/0.3	-87.2/-75.7	74.4/191.2	3.7/1.4	8.3/4.8
UE4	~103/~9	-2.13/8.4	-42.9/-22.0	119.0/7.1	2.3/38.7	10.1/13.3
UE5	~500/~49	2.8/15.8	-58.6/-39.7	126.2/16.1	2.2/17.1	14.6/0.9
UE6	~1000/~105	-1.8/14.7	-76.1/-44.5	181.8/4.0	1.5/68.8	3.8/12.3

IV. USER PERFORMANCE EVALUATION

Table IV compares the peak received SNR and the optimal throughput based on optimal MCS selection (Table V) using the RBIR abstraction technique for median and cell-edge users located in locations 2 and 3 respectively (see Fig. 5). The UE3-Pico outperforms the UE3-Macro in terms of peak SNR and optimal throughput (22.3 Mbps). When the UE rotates from case 2 to 3, the UE3-Macro experiences a 75.5% increase in peak throughput (7.1 Mbps-12.4 Mbps). However, the peak throughput with the UE3-Pico remains the same (22.3 Mbps). Figs. 9 and 10 show the predicted BER for a median user in the pico and macrocells at test location 2. The UE rotates through 360° and the results are summarized in Fig. 11. It can be seen that for the UE3-Pico the overall variation in performance is small compared to the UE3-Macro.

V. CONCLUSIONS

Results show that at the cell edge the macrocell has increased sensitivity to antenna rotation compared to the picocell. Results indicate that picocells can be used to improve downlink throughput, particularly for cell-edge users, since the average received signal power and throughput are much higher.

ACKNOWLEDGEMENTS

Zuhanis Mansor would like to thank the Majlis Amanah Rakyat (MARA) and Universiti Kuala Lumpur (UniKL) for her postgraduate scholarship. The authors acknowledge Centre for Communication Research, University of Bristol, for the provision of laboratory facilities and computing.

TABLE IV: PICO-UE /MACRO-UE PERFORMANCE FOR CASE 1, 2 & 3.

Location	Peak SNR (dB)	Optimal Throughput (Mbps)	MCS
UE2-Pico	26.6	24.12/24.07/35.63	5/5/6
UE3-Pico	18.8	15.64/22.3/22.3	3/4/4
UE2-Macro	34.4	43.0/42.95/41.83	7/7/7
UE3-Macro	7.3	7.72/7.06/12.39	1/1/2

TABLE V: LIST OF MCS MODES

	QPSK 1/2, 3/4	16QAM 1/2, 3/4	64QAM 3/4. 6/7
MCS	1,2	3,4	5,6

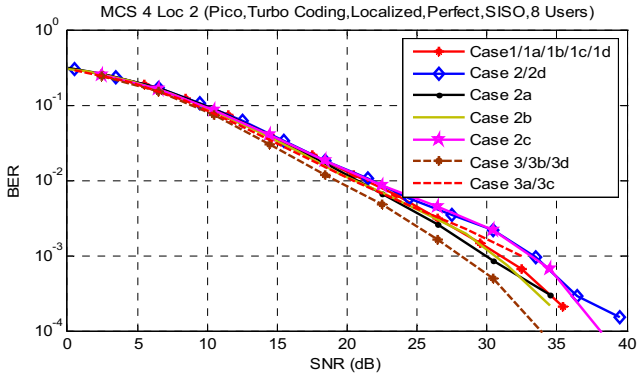

Figure 9: BER vs. SNR performance as users rotates through 360° for UE2-Pico at MCS 4.

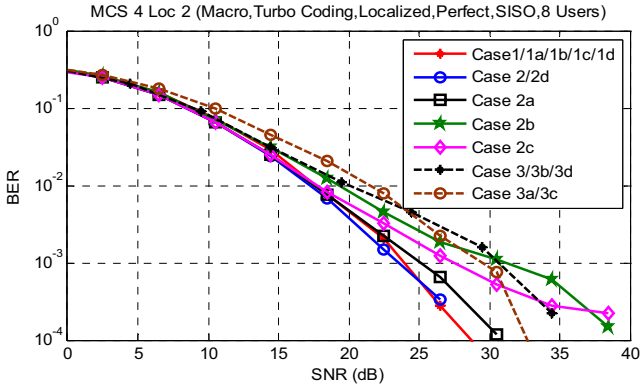

Figure 10: BER vs. SNR performance as users rotates through 360° for UE2-Macro at MCS 4.

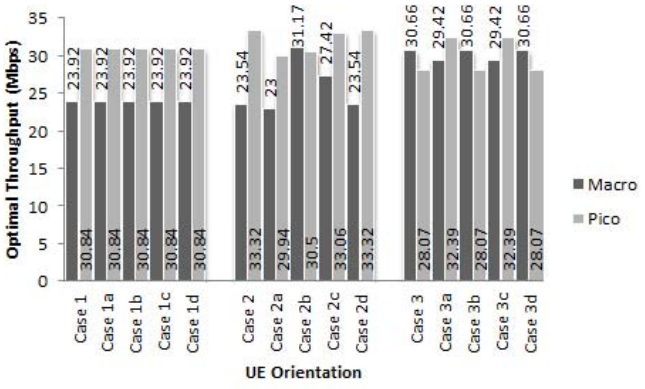

Figure 11: Peak pico and macrocell throughput as users rotates through 360° at location 2.

REFERENCES

[1] White Paper, "Global Mobile Data Traffic Forecast Update, 2010-2015", Cisco Visual Networking Index, February 2011.

[2] F. Athley and M. N. Johansson, "Impact of Electrical and Mechanical Antenna Tilt on LTE Downlink System Performance," IEEE 71st Vehicular Technology Conference, pp. 1-5, 2010.

[3] D. Kong, E. Mellios, D. Halls, A. R. Nix, and G. Hilton, "Closed-loop Antenna Selection for Wireless LANs with Directional & Omni- Directional Elements," accepted in Vehicular Technology Conference Fall, 2011.

[4] 3GPP TSG-RAN-WGI, "Evolved Universal Terrestrials Radio Access (E-UTRA): Further Advancements for E-UTRA Physical Layer Aspects," 3GPP, Tech. Rep. TR 36.814, 2010.

[5] R. Moray, LTE and the Evolution to 4G Wireless: Design and Measurement Challenges, Agilent Technologies, pp. 278-279, 2009.

[6] L. Wan, S. Tsai, and M. Almgren, "A Fading Insensitive Performance Metric for a Unified Link Quality Model," IEEE WCNC, April 2006.

[7] D. Halls, A.R. Nix and M.A. Beach, "System Level Evaluation of UL and DL Interference in OFDMA," IEEE WCNC, May, 2011.

[8] J. Wu, Z. Yin, J. Zhang and W. Heng, "Physical Layer Abstraction Algorithms Research for 802.11n and LTE Downlink," ISSSE, vol. 1, pp. 1-4, 2011.

[9] K.H. Ng, E.K. Tameh, A. Doufexi, M. Hunukumbure and A.R. Nix, "Efficient Multi-element Ray Tracing With Site-Specific Comparisons Using Measured MIMO Channel Data", IEEE Transactions on Vehicular Technology, Vol. 56, Issue 3, pp. 1019-1032, May 2007.

[10] 3GPP TR 25.996 Release 8, "Universal Mobile Telecommunications System (UMTS) Spatial Channel Model for Multiple Input Multiple Output (MIMO) Simulations," TR 125 996, pp. 0-41, 2009.

[11] Text Proposal R1-084026, "Evaluation Methodology Proposed for LTE-A," 3GPP TSG-RAN WG1, September-October 2008.

[12] C.A. Balanis, Antenna Theory: Analysis and Design, 2nd ed., John Wiley & Sons Inc., pp. 133-143, 1997.

[13] Y. Q Bian, A.R. Nix, E.K Tameh and J.P McGeehan, "MIMO–OFDM WLAN Architectures, Area Coverage, and Link Adaptation for Urban Hotspots," IEEE Trans. Veh. Tech, vol. 57, no. 4, July 2008.